AMERICAN SOCIETY FOR MICROBIOLOGY | Applied and Environmental Microbiology®

GEOMICROBIOLOGY

Meta-omics Reveal *Gallionellaceae* and *Rhodanobacter* Species as Interdependent Key Players for Fe(II) Oxidation and Nitrate Reduction in the Autotrophic Enrichment Culture KS

Yu-Ming Huang,[a,c] Daniel Straub,[a,b] Nia Blackwell,[a] Andreas Kappler,[c,d] Sara Kleindienst[a]

[a]Microbial Ecology, Center for Applied Geoscience, University of Tübingen, Tübingen, Germany
[b]Quantitative Biology Center (QBiC), University of Tübingen, Tübingen, Germany
[c]Geomicrobiology, Center for Applied Geoscience, University of Tübingen, Tübingen, Germany
[d]Cluster of Excellence, EXC 2124, "Controlling Microbes to Fight Infections," University of Tübingen, Tübingen, Germany

ABSTRACT Nitrate reduction coupled to Fe(II) oxidation (NRFO) has been recognized as an environmentally important microbial process in many freshwater ecosystems. However, well-characterized examples of autotrophic nitrate-reducing Fe(II)-oxidizing bacteria are rare, and their pathway of electron transfer as well as their interaction with flanking community members remain largely unknown. Here, we applied meta-omics (i.e., metagenomics, metatranscriptomics, and metaproteomics) to the nitrate-reducing Fe(II)-oxidizing enrichment culture KS growing under autotrophic or heterotrophic conditions and originating from freshwater sediment. We constructed four metagenome-assembled genomes with an estimated completeness of ≥95%, including the key players of NRFO in culture KS, identified as *Gallionellaceae* sp. and *Rhodanobacter* sp. The *Gallionellaceae* sp. and *Rhodanobacter* sp. transcripts and proteins likely involved in Fe(II) oxidation (e.g., *mtoAB*, *cyc2*, and *mofA*), denitrification (e.g., *napGHI*), and oxidative phosphorylation (e.g., respiratory chain complexes I to V) along with *Gallionellaceae* sp. transcripts and proteins for carbon fixation (e.g., *rbcL*) were detected. Overall, our results indicate that in culture KS, the *Gallionellaceae* sp. and *Rhodanobacter* sp. are interdependent: while *Gallionellaceae* sp. fixes CO_2 and provides organic compounds for *Rhodanobacter* sp., *Rhodanobacter* sp. likely detoxifies NO through NO reduction and completes denitrification, which cannot be performed by *Gallionellaceae* sp. alone. Additionally, the transcripts and partial proteins of cbb_3- and aa_3-type cytochrome *c* suggest the possibility for a microaerophilic lifestyle of the *Gallionellaceae* sp., yet culture KS grows under anoxic conditions. Our findings demonstrate that autotrophic NRFO is performed through cooperation among denitrifying and Fe(II)-oxidizing bacteria, which might resemble microbial interactions in freshwater environments.

IMPORTANCE Nitrate-reducing Fe(II)-oxidizing bacteria are widespread in the environment, contribute to nitrate removal, and influence the fate of the greenhouse gases nitrous oxide and carbon dioxide. The autotrophic growth of nitrate-reducing Fe(II)-oxidizing bacteria is rarely investigated and not fully understood. The most prominent model system for this type of study is the enrichment culture KS. To gain insights into the metabolism of nitrate reduction coupled to Fe(II) oxidation in the absence of organic carbon and oxygen, we performed metagenomic, metatranscriptomic, and metaproteomic analyses of culture KS and identified *Gallionellaceae* sp. and *Rhodanobacter* sp. as interdependent key Fe(II) oxidizers in culture KS. Our work demonstrates that autotrophic nitrate reduction coupled to Fe(II) oxidation is not performed by an individual strain but is a cooperation of at least two members of the bacterial community in culture KS. These findings serve as a foundation for our understanding of nitrate-reducing Fe(II)-oxidizing bacteria in the environment.

Citation Huang Y-M, Straub D, Blackwell N, Kappler A, Kleindienst S. 2021. Meta-omics reveal *Gallionellaceae* and *Rhodanobacter* species as interdependent key players for Fe(II) oxidation and nitrate reduction in the autotrophic enrichment culture KS. Appl Environ Microbiol 87:e00496-21. https://doi.org/10.1128/AEM.00496-21.

Editor Jeremy D. Semrau, University of Michigan-Ann Arbor

Address correspondence to Sara Kleindienst, sara.kleindienst@uni-tuebingen.de.

Received 11 March 2021
Accepted 16 May 2021
Accepted manuscript posted online 21 May 2021
Published 13 July 2021

KEYWORDS nitrate reduction coupled to Fe(II) oxidation, *Gallionellaceae*, *Bradyrhizobium*, *Rhodanobacter*, metagenomics, metatranscriptomics, metaproteomics

Neutrophilic nitrate reduction coupled to iron(II) [Fe(II)] oxidation (NRFO) by nitrate-reducing Fe(II)-oxidizing bacteria is known as a vital biochemical process in different natural environments, such as sediments and soils (1–9). Nitrate-reducing Fe(II)-oxidizing bacteria can thrive under different conditions: autotrophic, with Fe(II) as the sole energy and electron source; mixotrophic, with Fe(II) and additional organic carbon as energy, electron, and carbon sources; and heterotrophic, with organic carbon as the sole energy and carbon source. Chemolithotrophic Fe(II)-oxidizing bacteria (FeOB) use both solid and dissolved Fe(II) as an electron donor (10) under either oxic conditions, i.e., microaerophilic FeOB, or anoxic conditions, i.e., nitrate-reducing FeOB (1, 11–13). Despite the current knowledge of NRFO, for instance, as studied using the autotrophic nitrate-reducing Fe(II)-oxidizing bacterial enrichment culture KS (1), the knowledge of whether autotrophic NRFO can be performed by an individual strain or requires cooperation between different strains remains elusive (14).

Culture KS originated from a freshwater ecosystem in Bremen, Germany, and was first published in 1996 (1). The community composition of culture KS was analyzed under autotrophic growth conditions [using Fe(II) and nitrate] and under heterotrophic conditions (using acetate and nitrate) (15, 16). Under autotrophic conditions, culture KS was found to be enriched for an unclassified FeOB *Gallionellaceae* sp., which dominated with almost 96% relative 16S rRNA gene sequence abundance. The most closely related organisms to this unclassified *Gallionellaceae* sp. are the microaerophilic FeOB, *Ferrigenium kumadai* strain An22 (16S rRNA gene sequence identity, 96.45%) (17) and *Sideroxydans lithotrophicus* strain ES-1 (16S rRNA gene sequence identity, 95.23%) (18) as well as another unclassified *Gallionellaceae* sp. (16S rRNA gene sequence identity, 97.88%) (19) from the novel autotrophic NRFO enrichment culture BP that originated from the same environment as culture KS, i.e., a freshwater ecosystem in Bremen. However, despite elaborate cultivation attempts, the unclassified *Gallionellaceae* sp. of culture KS has so far not been isolated (15, 16).

Metagenomic analysis of culture KS, including metagenome-assembled genomes (MAGs), uncovered several genes encoding protein complexes potentially involved in extracellular electron transfer (EET) pathways during neutrophilic Fe(II) oxidation (16). Among the genes were those encoding the outer membrane cytochrome *c* (*cyc2*) detected in marine microaerophiles (20, 21) as well as the porin-cytochrome *c* protein complexes *pcoAB* known for Fe(II) oxidation in *Pseudomonas aeruginosa* (22) and the *mtoAB* gene cluster shown in several microaerophiles, including *Gallionella* sp. strain ES-2 and *Sideroxydans* sp. strain ES-1 (16, 23–25). However, it remained largely unknown which genes and proteins are ultimately involved in NRFO. Furthermore, in culture KS, the full denitrification gene complex, which consists of the genes encoding the nitrate reductase (*narGHI*), the nitrite reductase (*nirK/S*), the nitric oxide reductase (*norBC*), and the nitrous oxide reductase (*nosZ*), was only found in the MAGs of the heterotrophic organisms, i.e., the *Bradyrhizobium* sp. and *Rhodanobacter* sp. (16). In contrast, in the *Gallionellaceae* sp. MAG of culture KS, only the genes *narGHI* and *nirK/S* were identified. This was unexpected since the product of nitrite reduction, nitric oxide (NO), is generally toxic to organisms without detoxification genes (16). Therefore, it remained unclear how the unclassified *Gallionellaceae* sp. in culture KS deals with this toxic compound and survives under this condition. Apart from NRFO genes, the carbon fixation gene encoding a form II ribulose 1,5-bisphosphate carboxylase/oxygenase (RuBisCO) was identified in the *Gallionellaceae* sp. MAG, and genes encoding form IC RuBisCO were identified in the *Rhizobium* sp., *Bradyrhizobium* sp., and *Rhodanobacter* sp. MAGs in culture KS (16). It was further shown that, unlike the *Bradyrhizobium* sp., the unclassified *Gallionellaceae* sp. in culture KS is capable of CO_2 fixation during Fe(II) oxidation, confirming its chemolithoautotrophic lifestyle (26). In addition, the unclassified *Gallionellaceae* sp. from culture KS possesses high-oxygen-affinity genes

(i.e., encoding cbb_3-type cytochrome *c* oxidase) and low-oxygen-affinity genes (i.e., encoding aa_3-type cytochrome *c* oxidase), which require low and high oxygen concentrations, respectively (16, 27). This indicates that the unclassified *Gallionellaceae* sp. in culture KS might have the ability to respire oxygen as a microaerophilic Fe(II) oxidizer; however, it remained unknown whether these cytochrome *c* oxidases are expressed.

Based on this previous work, several mechanisms were proposed for Fe(II) oxidation in culture KS. Yet, the individual roles of the culture KS community members in Fe(II) oxidation, CO_2 fixation, reduction of the individual N species, and potential oxygen respiration remained elusive. Therefore, the aims of this study were (i) to identify genes and proteins expressed by the FeOB and other community members of culture KS under autotrophic and heterotrophic conditions, (ii) to create a concept of interspecies interaction based on the expressed genes and proteins which enables survival under autotrophic NRFO conditions in culture KS, and (iii) to obtain information from these expressed genes and proteins, allowing the development of potential isolation strategies of the unclassified *Gallionellaceae* sp. from culture KS for future studies. To answer these questions, we applied a meta-omics approach (i.e., metagenomics, metatranscriptomics, and metaproteomics) to culture KS under autotrophic and heterotrophic conditions. The physiology of the culture and population dynamics in these experiments were furthermore determined by monitoring Fe(II), nitrate, and acetate consumption as well as cell counts and 16S rRNA gene amplicon sequencing.

RESULTS AND DISCUSSION

Physiology of culture KS. For the meta-omics approach, culture KS was grown under anoxic autotrophic or anoxic heterotrophic conditions. Under autotrophic conditions, 9.34 mM Fe(II) was oxidized with an average Fe(II) oxidation rate of 3.25 mM/day during the exponential growth phase (i.e., between days 1 and 4) (Fig. 1A). This co-occurred with a reduction of 2.18 mM nitrate and an average nitrate reduction rate of 0.77 mM/day, without detectable nitrite production (Fig. 1A), suggesting either a potentially rapid consumption of nitrite by the enzyme nitrite reductase (NirK/S) or the involvement of nitrite in abiotic Fe(II) oxidation. The average $Fe(II)_{oxidized}$/$nitrate_{reduced}$ stoichiometric ratio was 4.28, indicative of autotrophic NRFO, albeit at a ratio that is slightly lower than the previously reported $Fe(II)_{oxidized}$/$nitrate_{reduced}$ ratios of 4.5 to 4.8 (15). The theoretical stoichiometry, however, suggests that the $Fe(II)_{oxidized}$/$nitrate_{reduced}$ ratio should be around 5 or even greater than 5 if the electrons used for CO_2 fixation were also considered (28). We suggest two possible explanations for this phenomenon. First, the product of nitrate reduction might not only be the final end member of denitrification, i.e., N_2, but may also be one of the less reduced N intermediates, i.e., NO or N_2O, which potentially leads to greenhouse gas emission. Second, heterotrophs might contribute to nitrate reduction using the electrons not only from Fe(II) but also from the trace amount of organic carbon present in Milli-Q water (determined at 2.17 mg/liter; triplicate measurements) used for medium preparation. In our experiments, cell numbers increased from 5.16×10^5 cells/ml to 2.82×10^7 cells/ml within 3 days (Fig. 1B). Given that 1 mg/liter of dissolved organic carbon in Milli-Q water could in theory produce 2.5×10^6 cells/ml (see the calculation in the supplemental material), cell growth in our cultivation experiments clearly derive not only from the trace amount of organic carbon but mainly from carbon fixation using electrons donated from Fe(II).

Under autotrophic growth conditions, the microbial community composition revealed that the unclassified *Gallionellaceae* sp. dominated, with 95% to 98% relative 16S rRNA gene sequence abundance (Fig. 1B). Conversely, lower abundances were detected for the *Rhodanobacter* sp. (2% to 3%), *Bradyrhizobium* sp. (up to 1%), *Nocardioides* sp. (<1%), and another *Gallionella* sp. (<1%) (Fig. 1B), in agreement with previous studies (15, 16, 28). The total cell numbers and the relative abundance of the unclassified *Gallionellaceae* sp. were higher than in a previous growth and population dynamics study (15), which reported total cell growth from 4×10^4 cells/ml to 2×10^6 cells/ml and an increase in the

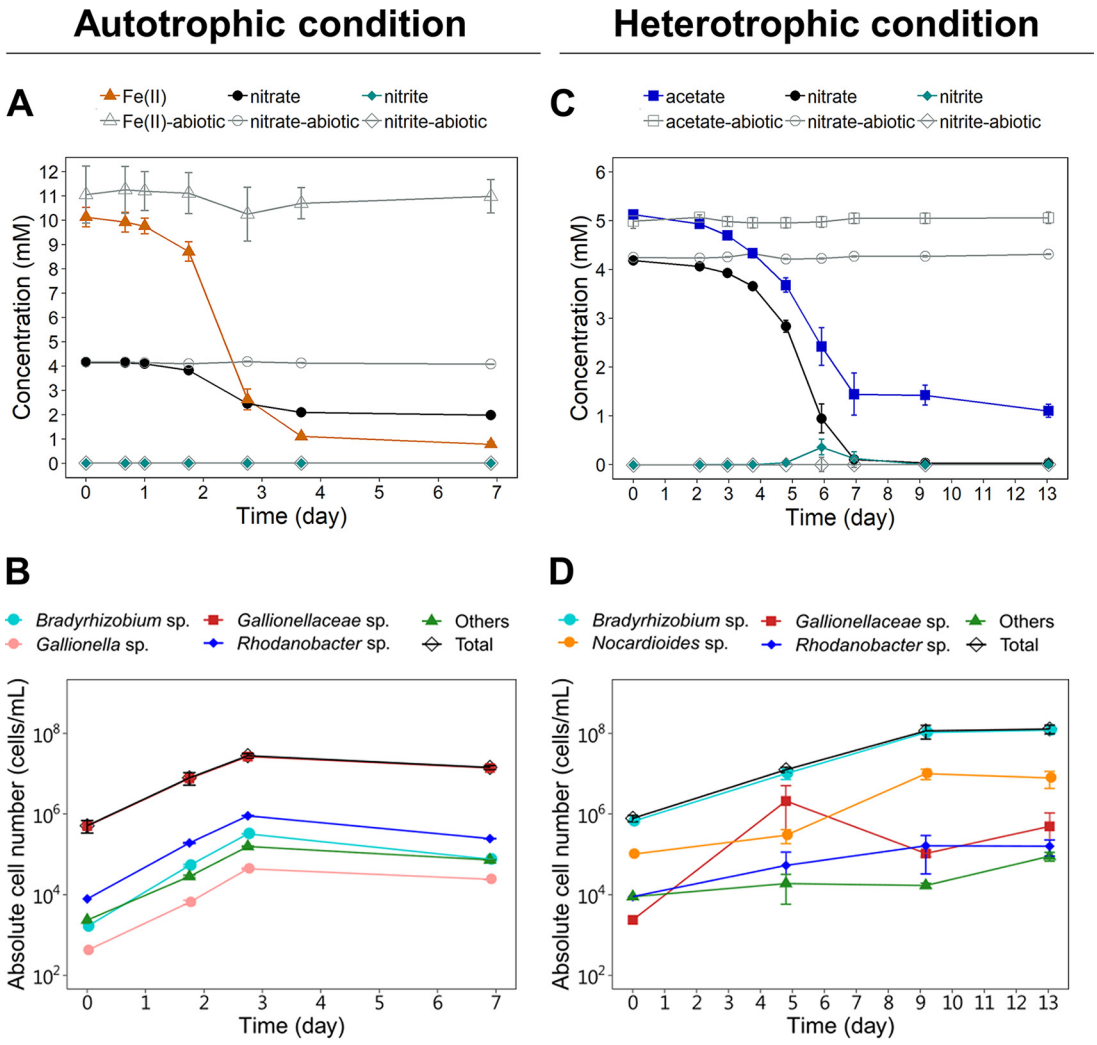

FIG 1 Geochemistry of culture KS under autotrophic (left) and heterotrophic (right) conditions. Changes in Fe(II), nitrate, and nitrite concentrations (A), acetate, nitrate, and nitrite concentrations (C), and estimated absolute cell numbers from total cell number (calculated with triplicate samples at all time points) and microbial community relative abundance of 16S rRNA gene amplicon sequencing (performed with triplicate samples, except for time zero) (B and D) as monitored over time. Error bars represent the standard deviations from three to four replicates (day 0 had no replicates in 16S rRNA gene amplicon sequencing).

unclassified *Gallionellaceae* sp. relative abundance from 58% to 83% in 10 days (15). In line with previous studies, the cell number increased 55 times over 3 days, and the unclassified *Gallionellaceae* sp. always accounted for the majority of the microbial community during the process of NRFO (Fig. 1B). Therefore, under autotrophic growth conditions, culture KS appeared reproducible, with only slight fluctuations among the different transfers.

Under heterotrophic conditions, 4.02 mM acetate was consumed with an average acetate oxidation rate of 0.72 mM/day during the exponential growth phase (i.e., between day 2 and day 7). This co-occurred with an average reduction of 4.16 mM nitrate and an average nitrate reduction rate of 0.82 mM/day. Nitrite was detected between day 4 and day 9 at concentrations ranging from 0.04 to 0.36 mM (Fig. 1C), pointing toward inefficient enzymatic nitrite reduction of the dominating microbial populations. The average $\text{acetate}_{\text{oxidized}}/\text{nitrate}_{\text{reduced}}$ ratio yield of 0.99 was similar to previously reported ratios (0.9 to 1.4) (15). Throughout the experiment, cell numbers increased from 7.85×10^5 cells/ml to 1.30×10^8 cells/ml within 9 days (Fig. 1D). The *Bradyrhizobium* sp. dominated under heterotrophic conditions, with 85% to 97% relative

16S rRNA gene sequence abundance, while lower abundances were detected for the *Nocardioides* sp. (3% to 13%), unclassified *Gallionellaceae* sp. (<1%), *Rhodanobacter* sp. (<1%), and *Pseudomonas* sp. (<1%) (Fig. 1D). Thus, the unclassified *Gallionellaceae* sp. and *Rhodanobacter* sp. were still detectable, albeit at low relative abundance (i.e., 0.09% to 0.38% and 0.08% to 1.13%, respectively).

Our data confirmed the population dynamics of the unclassified *Gallionellaceae* sp. and *Bradyrhizobium* sp. under heterotrophic and autotrophic conditions in culture KS, which have previously been determined via fluorescence *in situ* hybridization (FISH) (15), indicating that culture KS sustains a stable microbial consortium over time (i.e., several years). Our results also allowed us to determine optimal sampling points for meta-omics analysis, i.e., during the exponential growth phase of culture KS under both autotrophic and heterotrophic conditions.

Overview of the four assembled MAGs in culture KS under autotrophic and heterotrophic conditions. Four high-quality MAGs of the *Gallionellaceae* sp., *Rhodanobacter* sp., *Bradyrhizobium* sp., and *Nocardioides* sp. were recovered from the metagenomic data from culture KS with estimated completeness of ≥95% and estimated contamination of 0% (see Table S1). Several genes involved in carbon, nitrate, and oxygen metabolisms as well as in Fe(II) oxidation were identified (Fig. 2). Carbon metabolism pathway genes for the reductive pentose phosphate (CBB) cycle, the glycolysis pathway, tricarboxylic acid (TCA) cycle, and the pentose phosphate pathway (PPP) were identified in the four MAGs. Furthermore, the genes encoding RuBisCO were only identified in the MAGs of the *Gallionellaceae* sp. and *Bradyrhizobium* sp. but not in the *Rhodanobacter* sp., which is different from a previous report (16). The lack of RuBisCO in the *Rhodanobacter* sp. might be explained by evolutionary gene loss over time or incompleteness of the *Rhodanobacter* sp. MAG.

Regarding iron oxidation, the genes encoding outer membrane and porin-cytochrome *c* proteins of putative EET systems, i.e., *cyc2*, *mtoAB*, *pcoAB*, and outer membrane multi-copper oxidase (an *ompB* homolog, *mofA*), were detected in the MAGs of the *Gallionellaceae* sp. and *Rhodanobacter* sp., suggesting that both organisms might have the ability to oxidize Fe(II). Concerning the further electron acceptor pathway in the periplasm and inner membrane, the dissimilatory nitrate reductase complex *narGHI* and nitrite reductase *nirK/S* were detected in all four MAGs. The additional genes to complete denitrification, i.e., *norBC* and *nosZ*, were only detected in the MAGs of the *Rhodanobacter* sp., *Bradyrhizobium* sp., and *Nocardioides* sp. Another set of electron acceptors at the inner membrane of the cell are the oxidative phosphorylation complexes, i.e., the respiratory chain complexes I (NADH quinone oxidoreductase), II (succinate dehydrogenase), III (cytochrome bc_1 complex), IV (cbb_3- and aa_3-type cytochrome *c* oxidases), and V (F-type ATPase). We identified the genes encoding these oxidative phosphorylation systems in all four MAGs.

To determine the nutritional requirements of the bacterial populations in culture KS, particularly for the *Gallionellaceae* sp., we examined the amino acid biosynthesis pathways. The *Gallionellaceae* sp. MAG in culture KS encodes the complete synthesis pathways for the essential amino acids, suggesting that the *Gallionellaceae* sp. does not depend on other organisms regarding amino acid biosynthesis, which is in line with a previous metagenomic study (16).

Carbon fixation by the dominant *Gallionellaceae* sp. supports the survival of heterotrophic community members under autotrophic conditions. To advance the knowledge beyond the previous work (15, 16, 26, 28–30), we now also performed metatranscriptomic and metaproteomic analyses, which has not been performed with culture KS before. For a comparison of total transcript and protein abundances under autotrophic and heterotrophic conditions, differential abundance analysis was performed, which was the main basis of our interpretations (Fig. 2). In addition, normalized gene expression per MAG (i.e., *Gallionellaceae* sp., *Rhodanobacter* sp., *Bradyrhizobium* sp., and *Nocardioides* sp.) was calculated for both growth conditions using housekeeping genes as a reference and resulting in normalized transcripts per kilobase million (TPM) (see Fig. S1); however, these normalized results were interpreted with caution if data

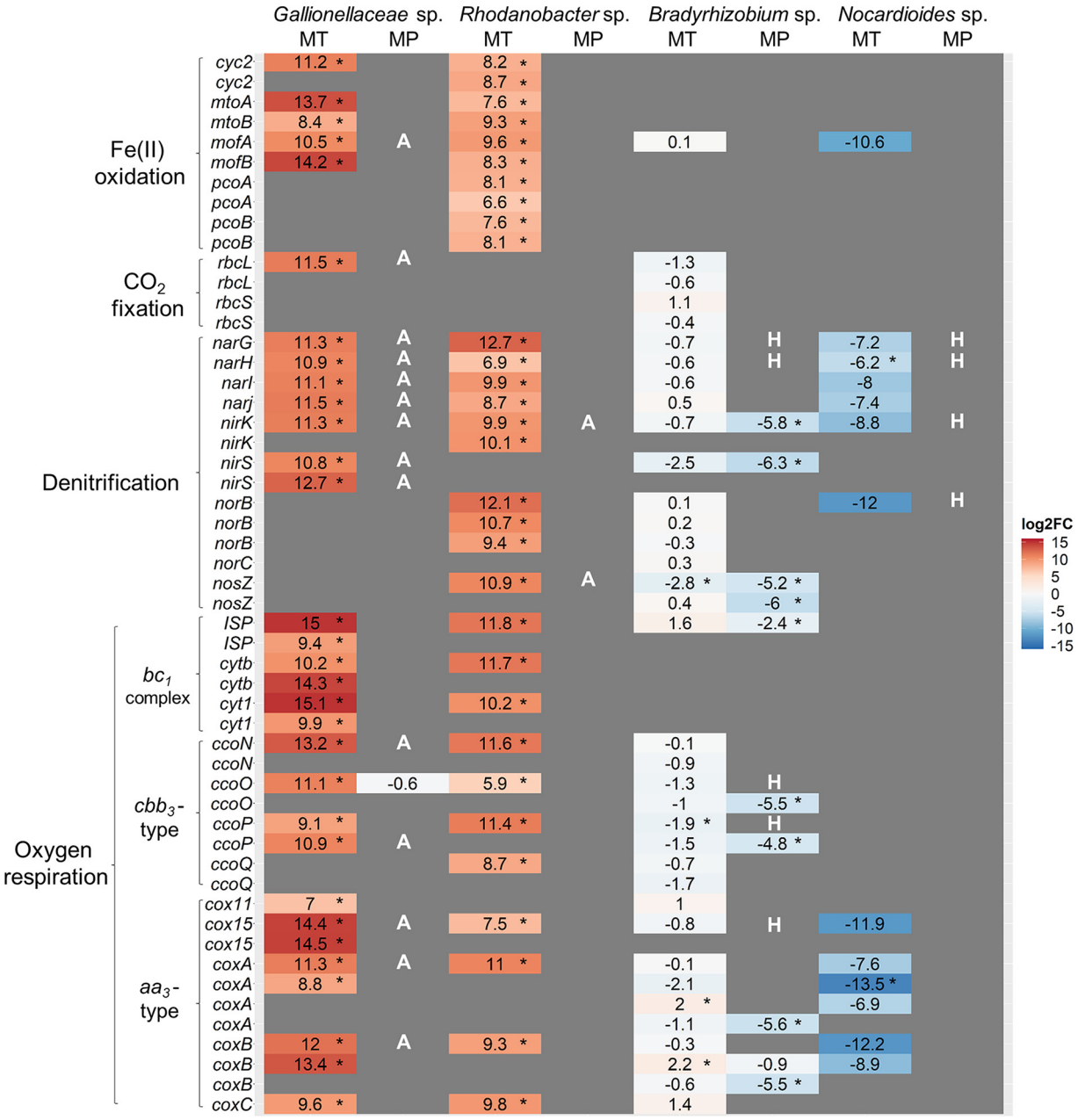

FIG 2 Fold changes of normalized counts (log_2) of key transcripts and proteins involved in Fe(II) oxidation, CO_2 fixation, acetate oxidation, denitrification, and potential oxygen respiration under autotrophic conditions compared to those under heterotrophic conditions. Genes with several copy numbers are listed multiple times. MT, metatranscriptomic analysis; MP, metaproteomic analysis. *, adjusted $P \leq 0.05$; A, protein was only detected under autotrophic conditions; H, protein was only detected under heterotrophic conditions.

were obtained from one sample only out of triplicates (a value of 0 TPM was interpreted as missing data). The metatranscriptomic analysis revealed the presence of several transcripts associated with carbon metabolic pathways under autotrophic NRFO conditions. Some of those transcripts showed significantly higher abundances under autotrophic conditions than under heterotrophic conditions (Fig. 2), more specifically, the essential carbon fixation gene transcripts, encoding form II RuBisCO (*rbcL*) and form IC RuBisCO (*rbcL/S*), of the *Gallionellaceae* sp. and *Bradyrhizobium* sp., respectively (Fig. 2). However, of these carbon fixation genes, only the *rbcL* transcript of the *Gallionellaceae* sp. was significantly ($P \leq 0.05$) more abundant under autotrophic conditions than under heterotrophic conditions, and the RbcL protein of the *Gallionellaceae* sp. was only detected under

autotrophic conditions (Fig. 2). In addition, the highest normalized gene expression of *rbcL* per MAG was calculated for the *Gallionellaceae* sp. under autotrophic conditions (4.78 averaged normalized TPM) (Fig. S1) and under heterotrophic conditions (however, with data from one sample only). In previous studies, form II RuBisCO was found in the nitrate-reducing FeOB *Thiobacillus denitrificans* as well as the microaerophilic FeOB *Sideroxydans lithotrophicus* ES-1 and *Gallionella capsiferriformans* ES-2 (23, 31). This gene usually has a low affinity to CO_2 and is adapted to high-CO_2 and low-O_2 environments; hence, it could function well under the anoxic bicarbonate-buffered cultivation conditions in culture KS (23, 32). Form IC RuBisCO was mostly found in the microorganisms living in environments with oxic conditions and reduced levels of CO_2 (32). Based on our findings, the expression level of form IC RuBisCO in the *Bradyrhizobium* sp. might rather be low under anoxic conditions (0 to 0.18 averaged normalized TPM per MAG) (Fig. S1), and this could explain why we were unable to detect the corresponding protein in our data set (Fig. 2). Our meta-omics data demonstrate, at both transcriptional and protein levels, that the *Gallionellaceae* sp. is the key organism responsible for carbon fixation under autotrophic conditions in culture KS (Fig. 3), supporting the hypothesis of Tominski et al., based on uptake studies of ^{13}C-labeled bicarbonate (26). In addition, under autotrophic conditions, we detected most of the transcripts and some of the proteins involved in the CBB cycle, the TCA cycle, the glycolysis pathway, and the PPP from the *Gallionellaceae* sp. and *Rhodanobacter* sp. (Fig. 2 and 3). Based on these detected carbon metabolism pathways, we propose that the *Gallionellaceae* sp. may proceed carbon fixation to produce the key component, i.e., organic carbon, 3-phosphoglycerate, for heterotrophic community members to survive under autotrophic conditions. These heterotrophs may subsequently metabolize 3-phosphoglycerate in the TCA cycle for further energy generation (Fig. 2) and for their survival in culture KS under autotrophic conditions. Hence, our data demonstrate that metabolic cooperation among microbial community members likely plays an essential role in the organic carbon-limited cultivation of the autotrophic culture KS, which might resemble the conditions in an organic carbon-poor aquifer (33) or even in a more organic carbon-rich coastal marine sediment (Norsminde, Denmark) (3).

The *Gallionellaceae* sp. and *Rhodanobacter* sp. likely perform Fe(II) oxidation in culture KS. The enzymatic Fe(II) oxidation by microaerophilic FeOB under pH-neutrophilic conditions has been proposed to occur at the outer membrane of the cell via EET instead of cytoplasmic Fe(II) oxidation to avoid intracellular mineral encrustation (9, 18, 29, 34, 35). Our transcriptomic data revealed that most of the detected putative EET system genes were expressed by the *Gallionellaceae* sp. and *Rhodanobacter* sp. (Fig. 2). For these two populations, the transcripts encoding Cyc2, MtoA, MtoB, Cytc1, Cytc2, Cytbc, and MofA were detected at a significantly higher abundance under autotrophic conditions than under heterotrophic conditions (Fig. 2). Additionally, in the *Rhodanobacter* sp., the transcripts encoding PcoA and PcoB were detected at significantly higher abundance levels under autotrophic conditions (Fig. 2). Furthermore, among the detected putative EET system transcripts, highest normalized gene expression per MAG was calculated for *cyc2* in the *Gallionellaceae* sp. (12.83 averaged normalized TPM) (Fig. S1) and for *pcoB* in the *Rhodanobacter* sp. (12.13 and 29.97 averaged normalized TPM of two *pcoB* copies) (Fig. S1) under autotrophic conditions. The normalized gene expression of *cyc2* in the *Gallionellaceae* sp. was also high under heterotrophic conditions; however, this was with data from one sample only. Homologs of the *mtoAB* and *cyc2* genes from the *Gallionellaceae* sp. in culture KS were found in the most closely related and publicly available genomes of *Sideroxydans lithotrophicus* ES-1 and *Gallionella capsiferriformans* ES-2 (16, 23, 36). MtoA and MtoB were shown to perform Fe(II) oxidation in the *Sideroxydans lithotrophicus* strain ES-1 (37). Furthermore, the *cyc2* gene encoding the putative Fe oxidase was identified in several FeOB genomes (36), *cyc2* transcripts were highly abundant *in situ* in *Zetaproteobacteria*-dominated Fe mats at marine hydrothermal vents (38), and *cyc2* transcripts as well as the Cyc2 protein were detected in the unclassified *Gallionellaceae* sp. of the novel autotrophic NRFO enrichment culture BP (19). Moreover, PcoA and PcoB were shown

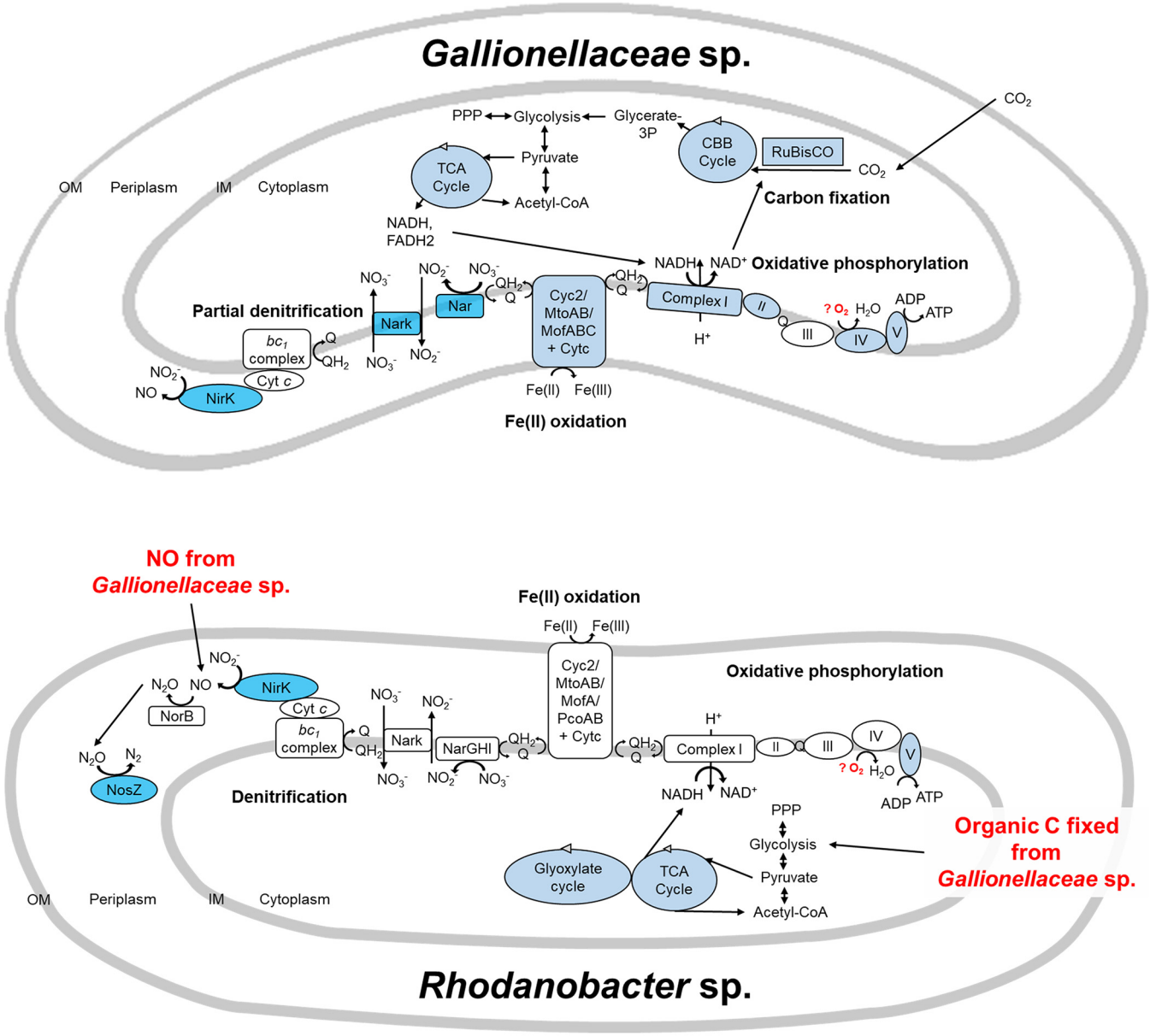

Proteins of incomplete pathway detected under autotrophic conditions

Proteins of complete pathway detected under autotrophic conditions

FIG 3 Overview of the proposed microbial interactions of the *Gallionellaceae* sp. and *Rhodanobacter* sp. in culture KS under autotrophic conditions. The depicted putative reactions are based on the meta-omics data for extracellular electron transfer system, denitrification, carbon metabolism, and oxidative phosphorylation in the *Gallionellaceae* sp. and *Rhodanobacter* sp. Most of the transcripts in this figure were detected under autotrophic conditions. Lighter blue color filling, incomplete pathway of proteins detected under autotrophic conditions; intense blue color filling, all proteins of the complete pathway detected under autotrophic conditions.

to use a broad range of redox substrates, and *pcoAB* homologs were widely identified in FeOB that have the genetic ability to oxidize Fe(II) (22, 36), e.g., in *P. aeruginosa*, for which the Fe(II) oxidation function of PcoA was demonstrated (22). It was therefore hypothesized that homologs of *pcoAB* might function in Fe(II) oxidation in many *Betaproteobacteria* (22, 36). The proteins MofA, MofB, and MofC were identified in *Leptothrix discophora* SS-1 and were speculated to be involved in Mn(II) and Fe(II)

oxidation (39–42). Under our growth conditions, no Mn(II) was added besides the trace amounts that originated from trace metals in the growth medium (0.50 μM); thus, it is unlikely that Mn(II) is the main electron donor in the KS culture, and we propose that the detected putative EET system transcripts are directly involved in Fe(II) oxidation. At the proteome level, we detected only the OmpB homolog MofA, which was assigned to the *Gallionellaceae* sp. MAG (Fig. 2). Even though we used a total protein extraction method, membrane proteins are difficult to extract (43), and we might have missed those EET proteins that reside in the membrane.

Collectively, the data from our meta-omics analyses combined with previous studies strengthen the concept that *cyc2*, *mtoAB*, *mofABC*, and *pcoAB* might be involved in EET to oxidize Fe(II) in not only the *Gallionellaceae* sp. but also the *Rhodanobacter* sp. (Fig. 2 and Fig. S1). However, according to the metaproteomic data, the *Gallionellaceae* sp. might be the key FeOB potentially employing MofA to oxidize Fe(II) and to transfer electrons from Fe(II) to the periplasm via MofB and MofC (36, 39, 41, 42). Indeed, the isolated *Rhodanobacter* sp. from culture KS was unable to oxidize $FeCl_2$ and Fe(II)-EDTA under either autotrophic or mixotrophic conditions (30). This indicates that the *Rhodanobacter* sp. might be dependent on the *Gallionellaceae* sp. to survive in culture KS under autotrophic conditions, as previously proposed (15, 16).

With respect to the other flanking community members under both autotrophic and heterotrophic conditions, the only EET transcripts detected for the *Bradyrhizobium* sp. and *Nocardioides* sp. were those of *mofA* (Fig. 2). The results overall indicate that the *Gallionellaceae* sp. might not depend on the *Rhodanobacter* sp. for the process of electron donation, i.e., Fe(II) oxidation, but might depend on the *Rhodanobacter* sp. for other metabolic steps, e.g., for accepting electrons from oxidation of organic carbon provided by the *Gallionellaceae* sp. at the periplasm and the inner membrane. Furthermore, in order to survive (and even grow) under carbon-limited and Fe(II)-rich conditions, heterotrophs such as the *Bradyrhizobium* sp. and *Nocardioides* sp. depend on the *Gallionellaceae* sp. that uses electrons from Fe(II) oxidation to fix carbon and, thus, provides organic compounds to the heterotrophs.

The *Rhodanobacter* sp. in culture KS likely detoxifies NO under autotrophic conditions. Among the processes able to accept the electrons donated by Fe(II) oxidation at the periplasm and the inner membrane of the bacterial populations in culture KS is the reduction of nitrate, also known as denitrification. The transcripts of the denitrification pathway genes, i.e., *narGHI* and *nirK/S* of the *Gallionellaceae* sp. as well as *narGHI*, *nirK*, *norB*, and *nosZ* of the *Rhodanobacter* sp., were detected at significantly higher abundances under autotrophic conditions (Fig. 2). The proteins NarGHI and NirK/S of the *Gallionellaceae* sp. as well as NirK and NosZ of the *Rhodanobacter* sp. were detected only under autotrophic conditions (Fig. 2). The *Rhodanobacter* sp. expressed all three copies of the nitric oxide reductase (*norB*) gene. In addition, normalized gene expression per MAG revealed highly expressed *norB* in the *Rhodanobacter* sp. under autotrophic conditions (439.88 averaged normalized TPM) (Fig. S1). Therefore, the *Rhodanobacter* sp. might play a role in NO detoxification, which is critical for the survival of the *Gallionellaceae* sp. (Fig. 2). It was previously suggested that the NO produced by the *Gallionellaceae* sp. could be reduced either via biotic processes by flanking community members or via abiotic processes, i.e., nitric oxide reduction coupled to Fe(II) oxidation (16). Based on our findings, the biotic process of NO detoxification by the *Rhodanobacter* sp. seems likely and might be essential for the survival of the *Gallionellaceae* sp. in the presence of toxic NO. This implies that the lack of the *nor* gene could be the barrier that prevents isolation of the *Gallionellaceae* sp. from culture KS. Thus, constant removal of NO may help for the isolation of the *Gallionellaceae* sp. in culture KS. Furthermore, the product derived from NO reduction is a greenhouse gas, N_2O, which is harmful to the environment. The proteins required for completing the denitrification pathway—NosZ by the *Rhodanobacter* sp. and the other heterotrophic community members—were detected in culture KS under autotrophic conditions, further highlighting the critical role of interspecies interactions in the process of reducing N_2O. In naturally occurring microbial communities, the

process of complete denitrification is vital to decrease N_2O greenhouse gas emissions which derive from incomplete microbial denitrification.

Oxidative phosphorylation pathway under anoxic conditions. Oxidative phosphorylation could also take part in accepting the electrons and transfer the electrons at the inner membrane to generate cellular energy. The metatranscriptome analysis revealed the presence of significantly higher abundances of oxidative phosphorylation gene transcripts under autotrophic compared to heterotrophic conditions for both, the *Gallionellaceae* sp. and *Rhodanobacter* sp. (Fig. 2). In addition, normalized gene expression per MAG showed high expression of *cytB* in the *Gallionellaceae* sp. (up to 34.31 averaged normalized TPM) (Fig. S1) and of *ccoQ* in the *Rhodanobacter* sp. (142.16 averaged normalized TPM) (Fig. S1) under autotrophic conditions. Interestingly, the *Gallionellaceae* sp. homologous proteins for the cbb_3- and aa_3-type cytochrome *c* oxidases of complex IV, which have high and low affinity to oxygen, respectively (27), were detected under autotrophic conditions (Fig. 2). These cbb_3- and aa_3-type cytochrome *c* oxidases are typically found in microaerophilic FeOB, such as *Sideroxydans lithotrophicus* strain ES-1, and aerobic acidophilic FeOB, such as *Acidithiobacillus ferrooxidans*, respectively (23, 44). Under heterotrophic conditions, only the transcripts of the *Bradyrhizobium* sp. genes encoding the protein complexes II, IV, and V were detected, and only a few of them had significantly higher abundances than under autotrophic conditions (Fig. 2). Furthermore, normalized gene expression per MAG revealed high levels of *ccoQ* in the *Bradyrhizobium* sp. (0.65 to 73.50 averaged normalized TPM) (Fig. S1) and of *coxB* in the *Nocardioides* sp. (369.27 to 579.49 averaged normalized TPM) (Fig. S1) under both growth conditions. These data suggest that under both growth conditions, oxidative phosphorylation with O_2 as an electron acceptor might occur in culture KS. However, our growth experiments were performed under anoxic conditions using N_2/CO_2 in the headspace and amended with $FeCl_2$ prior to inoculation, which would have consumed any atmospheric O_2 contamination during the preparation procedure. Hypothetically, there might be a similar mechanism as proposed for the nitric oxide reductase (Nod). Nod was suggested to produce oxygen and dinitrogen in aerobic methane-oxidizing bacteria under anoxic conditions (45), and the corresponding gene was widely detected in the environment (45–48). However, evidence of *nod* gene homologs was confirmed to be vague in culture KS, and the most similar protein in culture KS, compared to the published *nod* genes, has only 34% amino acid identity (in the *Rhodanobacter* sp.). Hence, to confirm the production of O_2 by an enzyme similar to Nod or the production of reactive oxygen species such as hydroxyl radicals, superoxide, and hydrogen peroxide in the culture KS system, further physiological experiments are required, as already suggested in a previous study (49). Another possible scenario might be constitutive expression of the oxidative phosphorylation complex III genes.

Overall, the microorganisms in culture KS may in theory have a microaerophilic living style, and the electrons accepted from the EET system may be transferred not only to the denitrification pathway but also to the oxidative phosphorylation pathway (Fig. 3). Indeed, several microoxic cultivation approaches, e.g., gradient tube and zero-valent iron plate, were used to grow culture KS and to isolate the *Gallionellaceae* sp. (15, 28). It was found that under these microoxic conditions, the *Gallionellaceae* sp. grew for the first few transfers, but the growth was not as stable as the culture under autotrophic anoxic NRFO conditions (15, 30), suggesting that the *Gallionellaceae* sp. prefers an autotrophic anoxic NRFO environment or requires the microbial network that thrives under these conditions.

Conclusion. Overall, our meta-omics analysis demonstrated that the microbial mechanism of NRFO occurs in the neutrophilic autotrophic enrichment culture KS at the transcript and protein levels. Based on this, both the *Gallionellaceae* sp. and *Rhodanobacter* sp. likely take part in the processes of Fe(II) oxidation and denitrification (Fig. 3). Carbon fixation by the *Gallionellaceae* sp. is probably required for the survival of the *Rhodanobacter* sp. (Fig. 3). In return, the *Rhodanobacter* sp. likely removes the toxic product, NO, that the *Gallionellaceae* sp. produces through incomplete

denitrification (Fig. 3). This indicates that the *Gallionellaceae* sp. and *Rhodanobacter* sp. have established a symbiotic relationship to survive in the organic carbon source-limited but Fe(II)- and nitrate-rich environment of culture KS under autotrophic conditions. While we cannot provide direct proof of enzymatic NRFO and NO detoxification, our meta-omics analysis strengthens previous evidence of these mechanisms and sheds more light on the fascinating metabolisms and interdependencies of the microbial key players in culture KS. Furthermore, our meta-omics analysis revealed transcripts and proteins in culture KS that are an important basis for follow-up studies. For instance, our data provide hints on the conditions that might be required to isolate the nitrate-reducing Fe(II)-oxidizing *Gallionellaceae* sp. One promising approach employs a growth chamber with a periplasm membrane in between, which might be used to grow the isolated *Rhodanobacter* sp. and the *Gallionellaceae* sp. via serial dilution from culture KS. This method would allow chemicals (e.g., organic carbon and NO) to pass through the membrane while separating the two species, resulting in a co-culture with complete pathways of NRFO and carbon fixation. Considering the environmental impact of microbial NRFO, a better knowledge of the physiology and the metabolism of members of the culture KS will be additionally valuable for the understanding of NRFO processes in the natural environment, particularly in organic carbon-limited but Fe(II)- and nitrate-containing habitats, such as aquifers. This knowledge may furthermore be used for treatment strategies of contaminated groundwater, wastewaters (50–52), or constructed wetlands (i.e., wastewater treatment systems) (53).

MATERIALS AND METHODS

Cultivation, analytical methods, and cell counts. Culture KS originates from a freshwater pond in Bremen, Germany (1). Since then, culture KS has been transferred for more than 20 years under autotrophic conditions. For at least 3 years, culture KS was transferred with 1% (vol/vol) inoculum, including more than 10 transfers per year. The culture was grown in 58-ml serum bottles with 25 ml bicarbonate-buffered, anoxic unfiltered medium containing 10 mM $FeCl_2$, 4 mM $NaNO_3$, vitamins, and trace elements with a final pH of 6.9 to 7.2 (28, 54). The incubation temperature was 28°C without a light source and agitation, and the N_2/CO_2 ratio in the headspace was 90:10. Under heterotrophic conditions, 5 mM acetate was used instead of 10 mM $FeCl_2$ as the electron donor. The analytic methods used to determine the concentrations of Fe(II), Fe(total), nitrate, nitrite, and acetate as well as 4′,6-diamidino-2-phenylindole (DAPI) cell counts were described previously (15).

Experimental setup for meta-omics. To achieve a high-quality metagenome, we used a hybrid approach with both short-read (Illumina) and long-read (Nanopore) sequencing technologies. Also, to assemble genomes optimally that dominate under either autotrophic or heterotrophic growth conditions, we sequenced samples of both treatments. Therefore, metagenome samples were obtained at day 2 (Illumina) and 7 (Nanopore) under autotrophic conditions and at day 13 (Illumina) under heterotrophic conditions.

For the metatranscriptomics and metaproteomics analyses, both autotrophic and heterotrophic conditions were used with biological triplicates. Under autotrophic conditions, within 4 days on average, 80% of Fe(II) was oxidized and 75% of nitrate was reduced. Therefore, samples under autotrophic conditions were taken at the 2nd day [remaining Fe(II) and NO_3^- was 8.7 mM and 3.8 mM, respectively; 7.95×10^6 cells/ml]. Under heterotrophic conditions, in a first step, a preculture was grown for two transfers with 1% (vol/vol) inoculum for 10 days each, allowing more than seven generations under preculture conditions, considering an average doubling time of 1.5 days, to avoid carryover of signals from gene and protein expression under autotrophic conditions. In a second step, the 3rd transfer under heterotrophic conditions was used for the experimental setup: within 7 days, 72% of acetate was oxidized and 97.5% of nitrate was reduced. Therefore, samples under heterotrophic conditions were taken at the 5th day (remaining: acetate, 3.68 mM; NO_3^-, 2.84 mM; NO_2^-, 0.04 mM; 5.29×10^7 cells/ml).

Biomass sampling. At the sampling time points, biomass of culture KS with total cell numbers ranging from 10^9 to 10^{10} cells was collected under sterile conditions on cellulose filters (mixed-cellulose ester sterile filter membrane, 0.22-μm pore size, 47-mm filter diameter; Millipore) using vacuum filtration. The filters were cut into pieces and either stored in 15-ml falcon tubes at −80°C before proceeding with DNA and RNA extractions or stored in 50-ml falcon tubes at −80°C before proceeding with the protein extractions.

DNA and RNA coextraction. DNA/RNA coextraction was performed according to the protocol of Lueders et al. (55) with the following modifications: two tubes of "MP Bio Lysis Matrix E" beads were added to a 15-ml falcon tube including the filter pieces with the collected biomass. To disrupt the cells, 3.75 ml PB buffer (112.87 mM Na_2HPO_4 and 7.12 mM NaH_2PO_4) and 1.25 ml TNS buffer (500 mM Tris-HCl, 100 mM NaCl, and 10% [wt/vol] SDS) were added, followed by bead beating for 4 min on the vortex adapter (maximum power) at room temperature (RT). The following centrifugation steps were all at maximum speed ($7,197 \times g$; Eppendorf centrifuge 5430 with Rotor F35-6-30) at 4°C. All transfer steps were conducted on ice. The samples were centrifuged twice for 15 min and transferred to a new 15-ml falcon

tube in between centrifugation steps to obtain a clear supernatant. Then, the supernatant was split into new sterile 2-ml tubes (1 ml per tube) to proceed with phenol-chloroform-isoamyl alcohol and chloroform-isoamyl alcohol extractions according to Lueders et al. (55). Subsequently, all aqueous phases were pooled again into a new 15-ml tube for polyethylene glycol (with 30% [wt/vol] polyethylene glycol 6000 and 1.6 M NaCl) precipitation overnight. From the ethanol washing step, the extraction was conducted using a clean bench. The ethanol was removed carefully with a pipette with filter tips, and the pellet was dried at RT for ca. 10 min. The DNA/RNA pellet was dissolved in 20 to 50 μl diethyl pyrocarbonate (DEPC)-treated water with Invitrogen Ambion RNase inhibitor (40 unit/μl, 1 μl RNase inhibitor/40 μl) at RT for 30 min. For RNA samples, DNA digestion with a TURBO DNA-free kit was performed according to the user's manual protocol for rigorous treatment. Successful DNA removal was confirmed by 30-cycle PCR using universal bacterial primers (see below). All samples were stored at −80°C before sequencing.

Protein extraction. Protein extraction was performed according to the "protein extraction method B" described by Spät et al. (56) with the following modifications: 5 ml and 2 ml lysis buffer were added to the samples from autotrophic and heterotrophic conditions, respectively, to dissolve cell pellets. The samples were incubated for 10 min at 95°C in a water bath, vortexed briefly, chilled on ice with 2 min-intervals in total 5 times, and, subsequently, sonicated on ice for 30 s with an ultrasonic homogenizer (Bandelin Sonopuls) at output control 4 and 40% duty cycle. The lysate was centrifuged at 7,197 × *g* for 1 min at RT, and the supernatant was then transferred into several 1.5-ml Eppendorf tubes and centrifuged at 20,817 × *g* (Eppendorf centrifuge 5430 with a rotor holding 30 1.5/2.0-ml tubes) for 10 min at RT. Samples were pooled again into sterile 50-ml solvent-resistant tubes. After the 8:1 acetone-methanol precipitation and incubation step overnight, the precipitate was washed with 5 ml ice-cold 80% (vol/vol) acetone in water and centrifuged at 7,197 × *g* for 5 min at 4°C. The protein pellets were air dried at RT and later dissolved in urea buffer and stored at −20°C.

Illumina 16S rRNA amplicon sequencing. Bacterial 16S rRNA genes were amplified using universal primers, i.e., 515f, GTGYCAGCMGCCGCGGTAA (57), and 806r, GGACTACNVGGGTWTCTAAT (58), fused to Illumina adapters. The PCR cycling conditions were as follows: 95°C for 3 min, 25 or 30 cycles of 95°C for 30 s, 55°C for 30 s, and 75°C for 30 s, followed by a final elongation step at 72°C for 3 min. The quality of the purified amplicons was determined using agarose gel electrophoresis. Subsequent library preparation steps, i.e., Nextera 2nd step PCR, including pooling and sequencing, were performed on an Illumina MiSeq sequencing system (Illumina, San Diego, CA, USA) using the 2 by 250-bp MiSeq reagent kit v2 by Microsynth AG (Balgach, Switzerland). Between 68,651 and 219,333 sequencing read pairs were generated for each sample. Quality control, reconstruction of 16S rRNA gene sequences, and taxonomic annotation were performed with nf-core/ampliseq v1.1.0 (59, 60) with Nextflow v20.04.1 (61) using containerized software with singularity v3.0.3 (62). Primers were trimmed, and untrimmed sequences were discarded (<8%) with Cutadapt v1.16 (63). Adapter and primer-free sequences were imported into QIIME 2 version 2018.06 (64), their quality was checked with demux (https://github.com/qiime2/q2-demux), and they were processed with DADA2 version 1.6.0 (65) to eliminate PhiX contamination, trim reads (position 200 in forward reads and 160 in reverse reads), correct errors, merge read pairs, and remove PCR chimeras; ultimately, 164 amplicon sequencing variants (ASVs) were obtained across all samples. Alpha rarefaction curves were produced with the QIIME 2 diversity alpha-rarefaction plugin, which indicated that the richness of the samples had been fully observed. A naive Bayes classifier was fitted with 16S rRNA gene sequences extracted with the PCR primer sequences from the QIIME-compatible 99% identity-clustered SILVA v132 database (66). ASVs were classified by taxon using the fitted classifier (67). Two ASVs that classified as chloroplasts or mitochondria were removed, totaling to <0.1% relative abundance per sample, and the remaining ASVs had their abundances extracted by feature-table (https://github.com/qiime2/q2-feature-table).

Metagenome sequencing, assembly, and annotation. Library preparation and shotgun Illumina sequencing of culture KS grown under autotrophic and heterotrophic conditions were performed by CeGaT, Tübingen, Germany. One microgram of DNA was used for library preparation with the TruSeq DNA PCR-free kit from Illumina without modifications. Libraries were sequenced on the Illumina NovaSeq 6000 platform to generate paired-end (2 by 150-bp) reads; 55.8 and 48.8 Gbp raw sequences were generated for autotrophic and heterotrophic growth conditions, respectively. Nanopore sequencing (Oxford Nanopore Technologies [ONT]) on culture KS under autotrophic conditions was performed by the NGS Competence Center Tübingen (NCCT) at the University of Tübingen, Germany. The DNA concentration was measured with a Qubit 4.0 dsDNA BR assay kit and a Nanodrop. The library was prepared according to the standard protocol of ONT. A PromethION flow cell (version 9.4.1) was loaded and run for 72 h with standard settings (base calling with high accuracy [HAC] mode, bias voltage of −180 mV) (68, 69), producing 53 Gbp in 5 million reads.

Short- and long-read quality control, hybrid assembly, metagenome assembled genome binning, and taxonomic annotation were performed with nf-core/mag v1.0.0 (https://nf-co.re/mag, https://zenodo.org/record/3589528#.YKetqnmSmF4) (60) with Nextflow v20.04.1 (61) using containerized software with singularity v3.0.3 (62). Short-read quality was assessed with FastQC v0.11.8 (70), quality filtering and Illumina adapter removal were performed with fastp v0.20.0 (71), and reads mapped with Bowtie 2 v2.3.5 (72) to the PhiX genome (enterobacteria phage WA11, GCA_002596845.1, ASM259684v1) were removed. Long-read quality was assessed with NanoPlot v1.26.3 (73), adapter trimming was performed with Porechop v0.2.3_seqan2.1.1 (https://github.com/rrwick/Porechop), *Escherichia* virus Lambda (PRJNA485481, GCA_000840245.1) contamination was removed with Nanolyse v1.1.0 (73), and quality filtering was performed with Filtlong v0.2.0 (https://github.com/rrwick/Filtlong) using short reads retaining 75% of all long reads (nf-core/mag parameters "–longreads_keep_percent 75 –longreads_length_weight 1"). Finally, processed short and long reads were assembled with metaSPAdes v3.13.1 (74), and the assembly was evaluated with QUAST v5.0.2 (75).

Metagenome assembled genomes (MAGs) were binned with MetaBAT 2 v2.13 (76) aided by the sequencing depth in libraries from autotrophic and heterotrophic conditions and checked for their completeness and contamination with BUSCO v3.0.2 (77) using 148 near-universal single-copy orthologs of bacteria (http://busco.ezlab.org/v3/datasets/bacteria_odb9.tar.gz) selected from OrthoDB v9 (78), summary statistics were obtained with QUAST for each MAG, and, finally, MAGs were taxonomically annotated with CAT v4.6 (79), using a reference database created 4 March 2020 from the NCBI nonredundant (nr) database using the "CAT prepare --fresh" command.

Characteristics of the assembled metagenome can be found in Table S2 in the supplemental material. Four high-quality metagenome-assembled genomes (MAGs) were obtained from the metagenome, with an estimated completeness of 95.3% to 99.3% and with no detectable contamination (Table S1).

The assembled metagenome and MAGs were uploaded in June 2020 to the Joint Genome Institute's Integrated Microbial Genome and Microbiome Expert Review (IMG/MER) pipeline (IMGAP v5.0.18) for annotation (available online at https://img.jgi.doe.gov/cgi-bin/mer/main.cgi; Chen et al. [80]). FeGenie (81), the National Center for Biotechnology Information (NCBI) BLAST function (https://blast.ncbi.nlm.nih.gov/Blast.cgi) (82), and the IMG database (80) were used to confirm potential Fe(II) oxidation genes. Metabolic pathways were searched by using the KEGG database (https://www.genome.jp/kegg/pathway.html) (83). GapMind was used for confirming complete gene pathways for essential amino acid biosynthesis (all with high confidence of the best gene candidate) (https://papers.genomics.lbl.gov/cgi-bin/gapView.cgi) (84). Table S3 lists the IMG accession numbers for genes of Fe(II) oxidation, carbon fixation, denitrification, and complex IV of oxidative phosphorylation from four MAGs of culture KS.

RNA sequencing, mapping, and differential RNA abundance. For metatranscriptomes, DNase treatment, library preparation including bacterial ribodepletion (with the NuGen universal prokaryotic RNA-Seq kit), and sequencing with 2 by 75 bp and 21 to 62 Mio clusters per sample were performed by Microsynth AG (Balgach, Switzerland) using triplicate samples of culture KS grown under autotrophic and heterotrophic conditions. For data analysis, nf-core/rnaseq v1.4.2 (https://nf-co.re/rnaseq) (59, 60) and its containerized software was used with singularity v3.0.3 (62). First, an index database adjusted to small genomes (--genomeSAindexNbases 10) was created with Spliced Transcripts Alignment to a Reference (STAR) v2.6.1d (85) on the IMGAP annotation of the metagenome. Next, nf-core/rnaseq was executed with Nextflow v20.04.1 (61) and performed the following: quality checks with FastQC v0.11.8 (70), removal of around 1% of base pairs per sample due to adapter contamination and trimming of low-quality regions with Trim Galore! v0.6.4, removal of 4% to 94% (average, 64%) of rRNA sequences with SortMeRNA v2.1b (86), alignment with STAR v2.6.1d of 93% to 95% and 46% to 74% reads for autotrophic and heterotrophic conditions, respectively, and finally summarization of 13.2 million to 16.8 million and 1.7 million to 16.3 million counts per sample for autotrophic and heterotrophic conditions, respectively, for genes by featureCounts v1.6.4 (87). Transcripts per kilobase million (TPM) (88) were calculated by StringTie v2.0 (89). For the comparison of total transcript abundances under autotrophic conditions and those under heterotrophic conditions, gene counts were used in differential abundance analysis in R v3.5.1 with DESeq2 v1.22.1, including median of ratios normalization (90), and a significant difference was postulated for transcripts with Benjamini and Hochberg adjusted P value of ≤ 0.05. Normalized gene expression (normalized TPM) per MAG was calculated according to a previous study (38). Reference genes were selected from the list of genes validated for constitutive expression (91), but the 16S rRNA gene was excluded from consideration given that we performed rRNA depletion. Further genes were excluded because they either were not detected in all MAGs or had undetectable expression (0 TPM) in all samples of at least one growth condition. Finally, the TPM values of the selected reference genes (*gapA*, *rpoA*, *rpoB*, *rpoC*, and *rpoD*) were averaged for each growth condition and MAG. Normalized TPM values for each gene were calculated by dividing its average TPM value per condition by the average TPM of the reference genes for the corresponding MAG and growth condition. For all calculations, a value of 0 TPM was treated as missing value. A summary of features of the metatranscriptome can be found in Fig. 2, Fig. S1, and Table S2.

Metaproteome analysis. The metaproteome analysis was conducted by the Quantitative Proteomics & Proteome Center, Tübingen (PCT) (92). Protein concentrations were determined via the Bradford assay (Bio-Rad) according to the user's manual. SDS-PAGE short gel purification (Invitrogen) was run, and in-gel digestion with trypsin was conducted as described previously (93). Extracted peptides were desalted using C_{18} StageTips (94) and subjected to liquid chromatography-tandem mass spectrometry (LC-MS/MS) analysis. LC-MS/MS analyses were performed on an Easy-nLC 1200 ultrahigh performance liquid chromatograph (UHPLC) (Thermo Fisher Scientific) coupled to an QExactive HF Orbitrap mass spectrometer (Thermo Fisher Scientific) as described elsewhere (92). Peptides were eluted with a 127-min segmented gradient at a flow rate of 200 nl/min, selecting 12 most intensive peaks for fragmentation with high-energy collisional dissociation (HCD). The MS data were processed with MaxQuant software suite 1.6.7.0 (95). The iBAQ and LFQ algorithms were enabled, and samples of the same treatment (autotrophic or heterotrophic conditions, respectively) were matched. Database search against protein sequences predicted by IMGAP on the metagenome assembly was performed using the Andromeda search engine (96). Overall, 41,819 peptides identified by MaxQuant were loaded with R package *proteus* v0.2.13 (97) (https://github.com/bartongroup/Proteus) in R v3.6.0 (98) (https://www.R-project.org/) and subsequently assigned to 5,833 proteins; accumulated protein intensities were normalized by each sample's median and transformed by $\log_2$. For the comparison of total protein abundances under autotrophic and heterotrophic conditions, differential protein abundance analysis was performed for the triplicates of autotrophic and heterotrophic conditions, and the significance level for rejecting the null hypothesis was set to 0.05. Key characteristics of the metaproteomes can be found in Fig. 2 and Table S2.

Data availability. The metagenome and MAGs are available through Integrated Microbial Genomes & Microbiomes (IMG) (https://img.jgi.doe.gov/), with the taxon identification (IMG genome identifier [ID]) 3300040739 for the culture KS metagenome and IMG genome IDs 2878407288, 2878409899, 2878413433, and 2878420039 for the MAGs of the *Gallionellaceae* sp., *Rhodanobacter* sp., *Bradyrhizobium* sp., and *Nocardioides* sp., respectively.

Raw sequencing data have been deposited with links to BioProject accession number PRJNA682552 in the NCBI BioProject database. The raw mass spectrometry proteomics data have been deposited to the ProteomeXchange Consortium via the PRIDE (99) partner repository with the data set identifier PXD023186. Accession numbers for each sample can be found in Table S4.

SUPPLEMENTAL MATERIAL

Supplemental material is available online only.

SUPPLEMENTAL FILE 1, PDF file, 0.7 MB.

ACKNOWLEDGMENTS

This work was supported by the German Research Foundation (Deutsche Forschungsgemeinschaft [DFG])-funded research training group RTG 1708 "Molecular principles of bacterial survival strategies." Daniel Straub was funded by the Institutional Strategy of the University of Tübingen (DFG, ZUK63). Nia Blackwell was funded by the Collaborative Research Center 1253 CAMPOS (project 5: fractured aquifers) from the DFG (grant number SFB 1253/1 2017). Andreas Kappler is funded by DFG under Germany's Excellence Strategy, Cluster of Excellence EXC 2124 (project ID 390838134). Sara Kleindienst is funded by an Emmy-Noether fellowship from the DFG (grant number 326028733).

We thank Irina Droste-Borel for metaproteomic analysis, Ellen Roehm for HPLC and continuous-flow analysis, Katrin Wunsch for DAPI cell counts, and Libera Lo-Presti and Katherine Thompson for manuscript draft review.

We declare no conflict of interest.

REFERENCES

1. Straub KL, Benz M, Schink B, Widdel F. 1996. Anaerobic, nitrate-dependent microbial oxidation of ferrous iron. Appl Environ Microbiol 62:1458–1460. https://doi.org/10.1128/AEM.62.4.1458-1460.1996.
2. Straub KL, Schönhuber WA, Buchholz-Cleven BEE, Schink B. 2004. Diversity of ferrous iron-oxidizing, nitrate-reducing bacteria and their involvement in oxygen-independent iron cycling. Geomicrobiol J 21:371–378. https://doi.org/10.1080/01490450490485854.
3. Laufer K, Røy H, Jørgensen BB, Kappler A. 2016. Evidence for the existence of autotrophic nitrate-reducing Fe(II)-oxidizing bacteria in marine coastal sediment. Appl Environ Microbiol 82:6120–6131. https://doi.org/10.1128/AEM.01570-16.
4. Straub KL, Buchholz-Cleven BE. 1998. Enumeration and detection of anaerobic ferrous iron-oxidizing, nitrate-reducing bacteria from diverse European sediments. Appl Environ Microbiol 64:4846–4856. https://doi.org/10.1128/AEM.64.12.4846-4856.1998.
5. Laufer K, Nordhoff M, Røy H, Schmidt C, Behrens S, Jørgensen BB, Kappler A. 2015. Coexistence of microaerophilic, nitrate-reducing, and phototrophic Fe(II) Oxidizers and Fe(III) reducers in coastal marine sediment. Appl Environ Microbiol 82:1433–1447. https://doi.org/10.1128/AEM.03527-15.
6. Benz M, Brune A, Schink B. 1998. Anaerobic and aerobic oxidation of ferrous iron at neutral pH by chemoheterotrophic nitrate-reducing bacteria. Arch Microbiol 169:159–165. https://doi.org/10.1007/s002030050555.
7. Shelobolina E, Konishi H, Xu H, Benzine J, Xiong MY, Wu T, Blothe M, Roden E. 2012. Isolation of phyllosilicate-iron redox cycling microorganisms from an illite-smectite rich hydromorphic soil. Front Microbiol 3:134. https://doi.org/10.3389/fmicb.2012.00134.
8. Hafenbradl D, Keller M, Dirmeier R, Rachel R, Rossnagel P, Burggraf S, Huber H, Stetter KO. 1996. *Ferroglobus placidus* gen. nov., sp. nov., a novel hyperthermophilic archaeum that oxidizes Fe^{2+} at neutral pH under anoxic conditions. Arch Microbiol 166:308–314. https://doi.org/10.1007/s002030050388.
9. Bryce C, Blackwell N, Schmidt C, Otte J, Huang YM, Kleindienst S, Tomaszewski E, Schad M, Warter V, Peng C, Byrne JM, Kappler A. 2018. Microbial anaerobic Fe(II) oxidation - ecology, mechanisms and environmental implications. Environ Microbiol 20:3462–3483. https://doi.org/10.1111/1462-2920.14328.
10. Ehrenberg CG. 1838. Die infusionsthierchen als vollkommene organismen: ein blick in das tiefere organische leben der natur. Verlag Leopold Voss, Leipzig, Germany.
11. Widdel F, Schnell S, Heising S, Ehrenreich A, Assmus B, Schink B. 1993. Ferrous iron oxidation by anoxygenic phototrophic bacteria. Nature 362:834–836. https://doi.org/10.1038/362834a0.
12. Emerson D. 2012. Biogeochemistry and microbiology of microaerobic Fe (II) oxidation. Biochem Soc Trans 40:1211–1216. https://doi.org/10.1042/BST20120154.
13. Hedrich S, Schlömann M, Johnson DB. 2011. The iron-oxidizing proteobacteria. Microbiology (Reading) 157:1551–1564. https://doi.org/10.1099/mic.0.045344-0.
14. Liu T, Chen D, Li X, Li F. 2019. Microbially mediated coupling of nitrate reduction and Fe(II) oxidation under anoxic conditions. FEMS Microbiol Ecol 95:fiz030. https://doi.org/10.1093/femsec/fiz030.
15. Tominski C, Heyer H, Lösekann-Behrens T, Behrens S, Kappler A. 2018. Growth and population dynamics of the anaerobic Fe(II)-oxidizing and nitrate-reducing enrichment culture KS. Appl Environ Microbiol 84:e02173-17. https://doi.org/10.1128/AEM.02173-17.
16. He S, Tominski C, Kappler A, Behrens S, Roden EE. 2016. Metagenomic analyses of the autotrophic Fe(II)-oxidizing, nitrate-reducing enrichment culture KS. Appl Environ Microbiol 82:2656–2668. https://doi.org/10.1128/AEM.03493-15.
17. Khalifa A, Nakasuji Y, Saka N, Honjo H, Asakawa S, Watanabe T. 2018. *Ferrigenium kumadai* gen. nov., sp. nov., a microaerophilic iron-oxidizing bacterium isolated from a paddy field soil. Int J Syst Evol Microbiol 68:2587–2592. https://doi.org/10.1099/ijsem.0.002882.
18. Emerson D, Moyer C. 1997. Isolation and characterization of novel iron-oxidizing bacteria that grow at circumneutral pH. Appl Environ Microbiol 63:4784–4792. https://doi.org/10.1128/AEM.63.12.4784-4792.1997.
19. Huang Y, Straub D, Kappler A, Smith N, Blackwell N, Kleindienst S. A novel enrichment culture highlights core features of microbial networks

contributing to autotrophic Fe(II) oxidation coupled to nitrate reduction. Microb Physiol, in press. https://doi.org/10.1159/000517083.
20. McAllister SM, Moore RM, Gartman A, Luther GW, Emerson D, Chan CS. 2019. The Fe(II)-oxidizing *Zetaproteobacteria*: historical, ecological and genomic perspectives. FEMS Microbiol Ecol 95:fiz015. https://doi.org/10.1093/femsec/fiz015.
21. Keffer KL, McAllister SM, Garber A, Hallahan BJ, Sutherland MC, Rozovsky S, Chan CS. 17 April 2021. Iron oxidation by a fused cytochrome-porin common to diverse Fe-oxidizing bacteria. bioRxiv https://doi.org/10.1101/228056.
22. Huston WM, Jennings MP, McEwan AG. 2002. The multicopper oxidase of *Pseudomonas aeruginosa* is a ferroxidase with a central role in iron acquisition. Mol Microbiol 45:1741–1750. https://doi.org/10.1046/j.1365-2958.2002.03132.x.
23. Emerson D, Field EK, Chertkov O, Davenport KW, Goodwin L, Munk C, Nolan M, Woyke T. 2013. Comparative genomics of freshwater Fe-oxidizing bacteria: implications for physiology, ecology, and systematics. Front Microbiol 4:254. https://doi.org/10.3389/fmicb.2013.00254.
24. Carlson HK, Clark IC, Melnyk RA, Coates JD. 2012. Toward a mechanistic understanding of anaerobic nitrate-dependent iron oxidation: balancing electron uptake and detoxification. Front Microbiol 3:57. https://doi.org/10.3389/fmicb.2012.00057.
25. Bethencourt L, Bochet O, Farasin J, Aquilina L, Borgne TL, Quaiser A, Biget M, Michon-Coudouel S, Labasque T, Dufresne A. 2020. Genome reconstruction reveals distinct assemblages of *Gallionellaceae* in surface and subsurface redox transition zones. FEMS Microbiol Ecol 96:fiaa036. https://doi.org/10.1093/femsec/fiaa036.
26. Tominski C, Lösekann-Behrens T, Ruecker A, Hagemann N, Kleindienst S, Mueller CW, Hoschen C, Kogel-Knabner I, Kappler A, Behrens S. 2018. Insights into carbon metabolism provided by fluorescence in situ hybridization-secondary ion mass spectrometry imaging of an autotrophic, nitrate-reducing, Fe(II)-oxidizing enrichment culture. Appl Environ Microbiol 84:e02166-17. https://doi.org/10.1128/AEM.02166-17.
27. Arai H, Kawakami T, Osamura T, Hirai T, Sakai Y, Ishii M. 2014. Enzymatic characterization and *in vivo* function of five terminal oxidases in *Pseudomonas aeruginosa*. J Bacteriol 196:4206–4215. https://doi.org/10.1128/JB.02176-14.
28. Blöthe M, Roden EE. 2009. Composition and activity of an autotrophic Fe(II)-oxidizing, nitrate-reducing enrichment culture. Appl Environ Microbiol 75:6937–6940. https://doi.org/10.1128/AEM.01742-09.
29. Nordhoff M, Tominski C, Halama M, Byrne JM, Obst M, Kleindienst S, Behrens S, Kappler A. 2017. Insights into nitrate-reducing Fe(II) oxidation mechanisms through analysis of cell-mineral associations, cell encrustation, and mineralogy in the chemolithoautotrophic enrichment culture KS. Appl Environ Microbiol 83:e00752-17. https://doi.org/10.1128/AEM.00752-17.
30. Tominski C. 2016. Genetic and physiological mechanisms of nitrate-dependent Fe(II) oxidation in the chemolithoautotrophic enrichment culture KS. PhD degree thesis. Eberhard Karls University of Tübingen, Tübingen, Germany.
31. Beller HR, Letain TE, Chakicherla A, Kane SR, Legler TC, Coleman MA. 2006. Whole-genome transcriptional analysis of chemolithoautotrophic thiosulfate oxidation by *Thiobacillus denitrificans* under aerobic versus denitrifying conditions. J Bacteriol 188:7005–7015. https://doi.org/10.1128/JB.00568-06.
32. Badger MR, Bek EJ. 2008. Multiple rubisco forms in proteobacteria: their functional significance in relation to CO_2 acquisition by the CBB cycle. J Exp Bot 59:1525–1541. https://doi.org/10.1093/jxb/erm297.
33. Jewell TNM, Karaoz U, Brodie EL, Williams KH, Beller HR. 2016. Metatranscriptomic evidence of pervasive and diverse chemolithoautotrophy relevant to C, S, N and Fe cycling in a shallow alluvial aquifer. ISME J 10:2106–2117. https://doi.org/10.1038/ismej.2016.25.
34. Carlson HK, Clark IC, Blazewicz SJ, Iavarone AT, Coates JD. 2013. Fe(II) oxidation is an innate capability of nitrate-reducing bacteria that involves abiotic and biotic reactions. J Bacteriol 195:3260–3268. https://doi.org/10.1128/JB.00058-13.
35. Kappler A, Schink B, Newman DK. 2005. Fe(III) mineral formation and cell encrustation by the nitrate-dependent Fe(II)-oxidizer strain BoFeN1. Geobiology 3:235–245. https://doi.org/10.1111/j.1472-4669.2006.00056.x.
36. He S, Barco RA, Emerson D, Roden EE. 2017. Comparative genomic analysis of neutrophilic iron(II) oxidizer genomes for candidate genes in extracellular electron transfer. Front Microbiol 8:1584. https://doi.org/10.3389/fmicb.2017.01584.
37. Liu J, Wang Z, Belchik SM, Edwards MJ, Liu C, Kennedy DW, Merkley ED, Lipton MS, Butt JN, Richardson DJ, Zachara JM, Fredrickson JK, Rosso KM, Shi L. 2012. Identification and characterization of MtoA: a decaheme *c*-type cytochrome of the neutrophilic Fe(II)-oxidizing bacterium *Sideroxydans lithotrophicus* ES-1. Front Microbiol 3:37. https://doi.org/10.3389/fmicb.2012.00037.
38. McAllister SM, Polson SW, Butterfield DA, Glazer BT, Sylvan JB, Chan CS. 2020. Validating the Cyc2 neutrophilic iron oxidation pathway using metaomics of *Zetaproteobacteria* iron mats at marine hydrothermal vents. mSystems 5:e00553-19. https://doi.org/10.1128/mSystems.00553-19.
39. Brouwers GJ, Corstjens PLAM, de Vrind A, Verkamman JPM, de Kuyper M, de Vrind-de Jong EW. 2000. Stimulation of Mn^{2+} oxidation in *Leptothrix discophora* SS-1 by Cu^{2+} and sequence analysis of the region flanking the gene encoding putative multicopper oxidase MofA. Geomicrobiol J 17:25–33.
40. Corstjens PLAM, de Vrind JPM, Goosen T, de Vrind-de Jong EW. 1997. Identification and molecular analysis of the *Leptothrix discophora* SS-1 *mofA* gene, a gene putatively encoding a manganese-oxidizing protein with copper domains. Geomicrobiol J 14:91–108. https://doi.org/10.1080/01490459709378037.
41. El Gheriany IA, Bocioaga D, Hay AG, Ghiorse WC, Shuler ML, Lion LW. 2009. Iron requirement for Mn(II) oxidation by *Leptothrix discophora* SS-1. Appl Environ Microbiol 75:1229–1235. https://doi.org/10.1128/AEM.02291-08.
42. Corstjens PL, de Vrind JP, Westbroek P, de Vrind-de Jong EW. 1992. Enzymatic iron oxidation by *Leptothrix discophora*: identification of an iron-oxidizing protein. Appl Environ Microbiol 58:450–454. https://doi.org/10.1128/AEM.58.2.450-454.1992.
43. Singer SJ. 1990. The structure and insertion of integral proteins in membranes. Annu Rev Cell Biol 6:247–296. https://doi.org/10.1146/annurev.cb.06.110190.001335.
44. Castelle C, Guiral M, Malarte G, Ledgham F, Leroy G, Brugna M, Giudici-Orticoni MT. 2008. A new iron-oxidizing/O_2-reducing supercomplex spanning both inner and outer membranes, isolated from the extreme acidophile *Acidithiobacillus ferrooxidans*. J Biol Chem 283:25803–25811. https://doi.org/10.1074/jbc.M802496200.
45. Ettwig KF, Butler MK, Le Paslier D, Pelletier E, Mangenot S, Kuypers MM, Schreiber F, Dutilh BE, Zedelius J, de Beer D, Gloerich J, Wessels HJ, van Alen T, Luesken F, Wu ML, van de Pas-Schoonen KT, Op den Camp HJ, Janssen-Megens EM, Francoijs KJ, Stunnenberg H, Weissenbach J, Jetten MS, Strous M. 2010. Nitrite-driven anaerobic methane oxidation by oxygenic bacteria. Nature 464:543–548. https://doi.org/10.1038/nature08883.
46. Hu Q-Q, Zhou Z-C, Liu Y-F, Zhou L, Mbadinga SM, Liu J-F, Yang S-Z, Gu J-D, Mu B-Z. 2019. High microbial diversity of the nitric oxide dismutation reaction revealed by PCR amplification and analysis of the nod gene. Int Biodeterior Biodegradation 143:104708. https://doi.org/10.1016/j.ibiod.2019.05.025.
47. Zhang Y, Ma A, Liu W, Bai Z, Zhuang X, Zhuang G. 2018. The occurrence of putative nitric oxide dismutase (nod) in an alpine wetland with a new dominant subcluster and the potential ability for a methane sink. Archaea 2018:6201541. https://doi.org/10.1155/2018/6201541.
48. Zhu B, Wang J, Bradford LM, Ettwig K, Hu B, Lueders T. 2019. Nitric oxide dismutase (*nod*) genes as a functional marker for the diversity and phylogeny of methane-driven oxygenic denitrifiers. Front Microbiol 10:1577. https://doi.org/10.3389/fmicb.2019.01577.
49. Mumford AC, Adaktylou IJ, Emerson D. 2016. Peeking under the iron curtain: development of a microcosm for imaging the colonization of steel surfaces by *Mariprofundus* sp. strain DIS-1, an oxygen-tolerant Fe-oxidizing bacterium. Appl Environ Microbiol 82:6799–6807. https://doi.org/10.1128/AEM.01990-16.
50. Su JF, Shi JX, Huang TL, Ma F, Lu JS, Yang SF. 2016. Effect of nitrate concentration, pH, and hydraulic retention time on autotrophic denitrification efficiency with Fe(II) and Mn(II) as electron donors. Water Sci Technol 74:1185–1192. https://doi.org/10.2166/wst.2016.231.
51. Zhang X, Li A, Szewzyk U, Ma F. 2016. Improvement of biological nitrogen removal with nitrate-dependent Fe(II) oxidation bacterium *Aquabacterium parvum* B6 in an up-flow bioreactor for wastewater treatment. Bioresour Technol 219:624–631. https://doi.org/10.1016/j.biortech.2016.08.041.
52. Kiskira K, Papirio S, van Hullebusch ED, Esposito G. 2017. Fe(II)-mediated autotrophic denitrification: a new bioprocess for iron bioprecipitation/biorecovery and simultaneous treatment of nitrate-containing wastewaters. Int Biodeterior Biodegradation 119:631–648. https://doi.org/10.1016/j.ibiod.2016.09.020.

53. Song X, Wang S, Wang Y, Zhao Z, Yan D. 2016. Addition of Fe^{2+} increase nitrate removal in vertical subsurface flow constructed wetlands. Ecol Eng 91:487–494. https://doi.org/10.1016/j.ecoleng.2016.03.013.
54. Hegler F, Posth NR, Jiang J, Kappler A. 2008. Physiology of phototrophic iron (II)-oxidizing bacteria: implications for modern and ancient environments. FEMS Microbiol Ecol 66:250–260. https://doi.org/10.1111/j.1574-6941.2008.00592.x.
55. Lueders T, Manefield M, Friedrich MW. 2004. Enhanced sensitivity of DNA- and rRNA-based stable isotope probing by fractionation and quantitative analysis of isopycnic centrifugation gradients. Environ Microbiol 6:73–78. https://doi.org/10.1046/j.1462-2920.2003.00536.x.
56. Spät P, Maček B, Forchhammer K. 2015. Phosphoproteome of the cyanobacterium *Synechocystis* sp. PCC 6803 and its dynamics during nitrogen starvation. Front Microbiol 6:248. https://doi.org/10.3389/fmicb.2015.00248.
57. Parada AE, Needham DM, Fuhrman JA. 2016. Every base matters: assessing small subunit rRNA primers for marine microbiomes with mock communities, time series and global field samples. Environ Microbiol 18:1403–1414. https://doi.org/10.1111/1462-2920.13023.
58. Apprill A, McNally S, Parsons R, Weber L. 2015. Minor revision to V4 region SSU rRNA 806R gene primer greatly increases detection of SAR11 bacterioplankton. Aquat Microb Ecol 75:129–137. https://doi.org/10.3354/ame01753.
59. Straub D, Blackwell N, Langarica-Fuentes A, Peltzer A, Nahnsen S, Kleindienst S. 2020. Interpretations of environmental microbial community studies are biased by the selected 16S rRNA (gene) amplicon sequencing pipeline. Front Microbiol 11:550420. https://doi.org/10.3389/fmicb.2020.550420.
60. Ewels PA, Peltzer A, Fillinger S, Patel H, Alneberg J, Wilm A, Garcia MU, Di Tommaso P, Nahnsen S. 2020. The nf-core framework for community-curated bioinformatics pipelines. Nat Biotechnol 38:276–278. https://doi.org/10.1038/s41587-020-0439-x.
61. Di Tommaso P, Chatzou M, Floden EW, Barja PP, Palumbo E, Notredame C. 2017. Nextflow enables reproducible computational workflows. Nat Biotechnol 35:316–319. https://doi.org/10.1038/nbt.3820.
62. Kurtzer GM, Sochat V, Bauer MW. 2017. Singularity: scientific containers for mobility of compute. PLoS One 12:e0177459. https://doi.org/10.1371/journal.pone.0177459.
63. Martin M. 2011. Cutadapt removes adapter sequences from high-throughput sequencing reads. EMBnet J 17:10–12. https://doi.org/10.14806/ej.17.1.200.
64. Bolyen E, Rideout JR, Dillon MR, Bokulich NA, Abnet CC, Al-Ghalith GA, Alexander H, Alm EJ, Arumugam M, Asnicar F, Bai Y, Bisanz JE, Bittinger K, Brejnrod A, Brislawn CJ, Brown CT, Callahan BJ, Caraballo-Rodríguez AM, Chase J, Cope EK, Da Silva R, Diener C, Dorrestein PC, Douglas GM, Durall DM, Duvallet C, Edwardson CF, Ernst M, Estaki M, Fouquier J, Gauglitz JM, Gibbons SM, Gibson DL, Gonzalez A, Gorlick K, Guo J, Hillmann B, Holmes S, Holste H, Huttenhower C, Huttley GA, Janssen S, Jarmusch AK, Jiang L, Kaehler BD, Kang KB, Keefe CR, Keim P, Kelley ST, Knights D, et al. 2019. Reproducible, interactive, scalable and extensible microbiome data science using QIIME 2. Nat Biotechnol 37:852–857. https://doi.org/10.1038/s41587-019-0209-9.
65. Callahan BJ, McMurdie PJ, Rosen MJ, Han AW, Johnson AJ, Holmes SP. 2016. DADA2: high-resolution sample inference from Illumina amplicon data. Nat Methods 13:581–583. https://doi.org/10.1038/nmeth.3869.
66. Pruesse E, Quast C, Knittel K, Fuchs BM, Ludwig W, Peplies J, Glockner FO. 2007. SILVA: a comprehensive online resource for quality checked and aligned ribosomal RNA sequence data compatible with ARB. Nucleic Acids Res 35:7188–7196. https://doi.org/10.1093/nar/gkm864.
67. Bokulich NA, Kaehler BD, Rideout JR, Dillon M, Bolyen E, Knight R, Huttley GA, Gregory Caporaso J. 2018. Optimizing taxonomic classification of marker-gene amplicon sequences with QIIME 2's q2-feature-classifier plugin. Microbiome 6:90. https://doi.org/10.1186/s40168-018-0470-z.
68. Moss EL, Maghini DG, Bhatt AS. 2020. Complete, closed bacterial genomes from microbiomes using nanopore sequencing. Nat Biotechnol 38:701–707. https://doi.org/10.1038/s41587-020-0422-6.
69. Goldstein S, Beka L, Graf J, Klassen JL. 2019. Evaluation of strategies for the assembly of diverse bacterial genomes using MinION long-read sequencing. BMC Genomics 20:23. https://doi.org/10.1186/s12864-018-5381-7.
70. Andrews S. 2010. FastQC: a quality control tool for high throughput sequence data. http://www.bioinformatics.babraham.ac.uk/projects/fastqc/.
71. Chen S, Zhou Y, Chen Y, Gu J. 2018. fastp: an ultra-fast all-in-one FASTQ preprocessor. Bioinformatics 34:i884–i890. https://doi.org/10.1093/bioinformatics/bty560.
72. Langmead B, Salzberg SL. 2012. Fast gapped-read alignment with Bowtie 2. Nat Methods 9:357–359. https://doi.org/10.1038/nmeth.1923.
73. De Coster W, D'Hert S, Schultz DT, Cruts M, Van Broeckhoven C. 2018. NanoPack: visualizing and processing long-read sequencing data. Bioinformatics 34:2666–2669. https://doi.org/10.1093/bioinformatics/bty149.
74. Nurk S, Meleshko D, Korobeynikov A, Pevzner PA. 2017. metaSPAdes: a new versatile metagenomic assembler. Genome Res 27:824–834. https://doi.org/10.1101/gr.213959.116.
75. Gurevich A, Saveliev V, Vyahhi N, Tesler G. 2013. QUAST: quality assessment tool for genome assemblies. Bioinformatics 29:1072–1075. https://doi.org/10.1093/bioinformatics/btt086.
76. Kang DD, Li F, Kirton E, Thomas A, Egan R, An H, Wang Z. 2019. MetaBAT 2: an adaptive binning algorithm for robust and efficient genome reconstruction from metagenome assemblies. PeerJ 7:e7359. https://doi.org/10.7717/peerj.7359.
77. Waterhouse RM, Seppey M, Simão FA, Manni M, Ioannidis P, Klioutchnikov G, Kriventseva EV, Zdobnov EM. 2018. BUSCO applications from quality assessments to gene prediction and phylogenomics. Mol Biol Evol 35:543–548. https://doi.org/10.1093/molbev/msx319.
78. Zdobnov EM, Tegenfeldt F, Kuznetsov D, Waterhouse RM, Simão FA, Ioannidis P, Seppey M, Loetscher A, Kriventseva EV. 2017. OrthoDB v9.1: cataloging evolutionary and functional annotations for animal, fungal, plant, archaeal, bacterial and viral orthologs. Nucleic Acids Res 45:D744–D749. https://doi.org/10.1093/nar/gkw1119.
79. von Meijenfeldt FAB, Arkhipova K, Cambuy DD, Coutinho FH, Dutilh BE. 2019. Robust taxonomic classification of uncharted microbial sequences and bins with CAT and BAT. Genome Biol 20:217. https://doi.org/10.1186/s13059-019-1817-x.
80. Chen IA, Chu K, Palaniappan K, Pillay M, Ratner A, Huang J, Huntemann M, Varghese N, White JR, Seshadri R, Smirnova T, Kirton E, Jungbluth SP, Woyke T, Eloe-Fadrosh EA, Ivanova NN, Kyrpides NC. 2019. IMG/M v.5.0: an integrated data management and comparative analysis system for microbial genomes and microbiomes. Nucleic Acids Res 47:D666–D677. https://doi.org/10.1093/nar/gky901.
81. Garber AI, Nealson KH, Okamoto A, McAllister SM, Chan CS, Barco RA, Merino N. 2020. FeGenie: a comprehensive tool for the identification of iron genes and iron gene neighborhoods in genome and metagenome assemblies. Front Microbiol 11:37. https://doi.org/10.3389/fmicb.2020.00037.
82. Altschul SF, Gish W, Miller W, Myers EW, Lipman DJ. 1990. Basic local alignment search tool. J Mol Biol 215:403–410. https://doi.org/10.1016/S0022-2836(05)80360-2.
83. Kanehisa M, Goto S. 2000. KEGG: Kyoto Encyclopedia of Genes and Genomes. Nucleic Acids Res 28:27–30. https://doi.org/10.1093/nar/28.1.27.
84. Price MN, Deutschbauer AM, Arkin AP. 2020. GapMind: automated annotation of amino acid biosynthesis. mSystems 5:e00291-20. https://doi.org/10.1128/mSystems.00291-20.
85. Dobin A, Davis CA, Schlesinger F, Drenkow J, Zaleski C, Jha S, Batut P, Chaisson M, Gingeras TR. 2013. STAR: ultrafast universal RNA-seq aligner. Bioinformatics 29:15–21. https://doi.org/10.1093/bioinformatics/bts635.
86. Kopylova E, Noe L, Touzet H. 2012. SortMeRNA: fast and accurate filtering of ribosomal RNAs in metatranscriptomic data. Bioinformatics 28:3211–3217. https://doi.org/10.1093/bioinformatics/bts611.
87. Liao Y, Smyth GK, Shi W. 2014. featureCounts: an efficient general purpose program for assigning sequence reads to genomic features. Bioinformatics 30:923–930. https://doi.org/10.1093/bioinformatics/btt656.
88. Li B, Dewey CN. 2011. RSEM: accurate transcript quantification from RNA-Seq data with or without a reference genome. BMC Bioinformatics 12:323. https://doi.org/10.1186/1471-2105-12-323.
89. Pertea M, Kim D, Pertea GM, Leek JT, Salzberg SL. 2016. Transcript-level expression analysis of RNA-seq experiments with HISAT, StringTie and Ballgown. Nat Protoc 11:1650–1667. https://doi.org/10.1038/nprot.2016.095.
90. Love MI, Huber W, Anders S. 2014. Moderated estimation of fold change and dispersion for RNA-seq data with DESeq2. Genome Biol 15:550. https://doi.org/10.1186/s13059-014-0550-8.
91. Rocha DJ, Santos CS, Pacheco LG. 2015. Bacterial reference genes for gene expression studies by RT-qPCR: survey and analysis. Antonie Van Leeuwenhoek 108:685–693. https://doi.org/10.1007/s10482-015-0524-1.

92. Schmitt M, Sinnberg T, Nalpas NC, Maass A, Schittek B, Macek B. 2019. Quantitative proteomics links the intermediate filament nestin to resistance to targeted BRAF inhibition in melanoma cells. Mol Cell Proteomics 18:1096–1109. https://doi.org/10.1074/mcp.RA119.001302.
93. Borchert N, Dieterich C, Krug K, Schutz W, Jung S, Nordheim A, Sommer RJ, Macek B. 2010. Proteogenomics of *Pristionchus pacificus* reveals distinct proteome structure of nematode models. Genome Res 20:837–846. https://doi.org/10.1101/gr.103119.109.
94. Rappsilber J, Mann M, Ishihama Y. 2007. Protocol for micro-purification, enrichment, pre-fractionation and storage of peptides for proteomics using StageTips. Nat Protoc 2:1896–1906. https://doi.org/10.1038/nprot.2007.261.
95. Cox J, Mann M. 2008. MaxQuant enables high peptide identification rates, individualized p.p.b.-range mass accuracies and proteome-wide protein quantification. Nat Biotechnol 26:1367–1372. https://doi.org/10.1038/nbt.1511.
96. Cox J, Neuhauser N, Michalski A, Scheltema RA, Olsen JV, Mann M. 2011. Andromeda: a peptide search engine integrated into the MaxQuant environment. J Proteome Res 10:1794–1805. https://doi.org/10.1021/pr101065j.
97. Gierlinski M, Gastaldello F, Cole C, Barton GJ. 20 September 2018. *Proteus*: an R package for downstream analysis of *MaxQuant* output. bioRxiv https://doi.org/10.1101/416511.
98. R Core Development Team. 2010. R: a language and environment for statistical computing. R Foundation for Statistical Computing, Vienna, Austria.
99. Perez-Riverol Y, Csordas A, Bai J, Bernal-Llinares M, Hewapathirana S, Kundu DJ, Inuganti A, Griss J, Mayer G, Eisenacher M, Pérez E, Uszkoreit J, Pfeuffer J, Sachsenberg T, Yilmaz S, Tiwary S, Cox J, Audain E, Walzer M, Jarnuczak AF, Ternent T, Brazma A, Vizcaíno JA. 2019. The PRIDE database and related tools and resources in 2019: improving support for quantification data. Nucleic Acids Res 47:D442–D450. https://doi.org/10.1093/nar/gky1106.